PAPER

Check for updates

Proteomics as a tool to study the osteoimmunomodulatory role of metallic ions in a sol–gel coating†

Iñaki García-Arnáez,‡*[a] Francisco Romero-Gavilán, [ID] ‡[b] Andreia Cerqueira, [ID] [b] Mikel Azkargorta,[c] Félix Elortza,[c] Julio Suay,[b] Isabel Goñi[a] and Mariló Gurruchaga [ID] *[a]

The success of bone implants depends on the osteoimmunomodulatory (OIM) activity of the biomaterials in the interactions with the periimplantary tissues. Many *in vitro* tests have been conducted to evaluate the osteoimmunology effects of biomaterials. However, results of these tests have often been inconclusive. This study examines the properties of newly developed sol–gel coatings doped with two metal ions associated with bone regeneration, Ca and Zn. The study uses both proteomic methods and traditional *in vitro* assays. The results demonstrate that proteomics is an effective tool to scrutinize the OIM properties of the materials. Moreover, sol–gel coatings offer excellent base materials to evaluate the effects of metal ions on these properties. The obtained data highlight the highly tunable nature of sol–gel materials; studying the materials with different doping levels supplies valuable information on the interactions between the immune and bone-forming processes.

1. Introduction

In recent years, the improved understanding of bone biology and the effects of the immune system on bone-remodeling has led to changes in research preferences. As a result, a new field, osteoimmunology, has emerged.[1] The term "osteoimmunology" was first used in 2000 when Arron and Choi[2] highlighted the relationship between the immune and skeletal systems, especially in autoimmune and other inflammatory diseases. More than a decade later, Chen *et al.*[3] proposed a new approach to the advanced bone-biomaterials design paradigm. They highlighted the importance of considering the role of immune responses while generating new bone biomaterials. Such materials should be able to modulate the local immune environment favoring the osteogenesis and osseointegration of the implant. The authors proposed the term "osteoimmunology" to define this process.

Recently, other authors[4] have reported that the success of bone implants depends on the osteoimmunological response provoked by the biomaterials. The traditional *in vitro* tests used to evaluate biomaterials may be replaced by more advanced and efficient approaches. Thus, techniques such as microarrays, bioreactors, and microfluidic-based systems emerge as alternatives.[4] These systems allow multiple all-in-one measurements that could offer improved physiologically relevant screening conditions. However, the first event after implantation, *i.e.* the inflammation, is triggered by forming a blood clot around the biomaterial and the adsorption of proteins on its surface. Thus, the analysis of the protein layer formed on biomaterials using proteomics is a powerful approach to provide the first key information on the pathways triggered by the different materials.[5] Therefore, proteomic studies should also be considered necessary for biomaterials development and validation.

Many biomaterials have been developed for their application in bone regeneration. The sol–gel materials based on Si have caught the attention of many researchers. These materials can enhance bone regeneration through the release of Si. They can also be employed as release vehicle of different molecules or metal ions to modulate their biological responses.[5,6] The physiological effects of some metallic elements on bone homeostasis have been already described. Ca and Zn are metals associated with similar biological pathways; they are implicated in regulating thousands of proteins.

Moreover, doping sol–gel coatings with Ca enhances their osteoinductive and coagulation properties in comparison with

[a] Departament of Polymers and Advanced Materials: Physics, Chemistry and Technology, Universidad del País Vasco, Po Manuel de Lardizábal, 3, 20018 San Sebastián, Spain. E-mail: marilo.gurruchaga@ehu.eus

[b] Department of Industrial Systems Engineering and Design, Universitat Jaume I, Av. Vicent Sos Baynat s/n, 12071 Castellón de la Plana, Spain

[c] Proteomics Platform, CIC bioGUNE, Basque Research and Technology Alliance (BRTA), CIBERehd, ProteoRed-ISCIII, Bizkaia Science and Technology Park, 48160 Derio, Spain

† Electronic supplementary information (ESI) available. See DOI: https://doi.org/10.1039/d3tb01204b

‡ Francisco Romero-Gavilán and Iñaki García-Arnáez equal contribution.

8194 | *J. Mater. Chem. B*, 2023, **11**, 8194–8205

This journal is © The Royal Society of Chemistry 2023

the bare coating.[6] Ca supports important functions of blood cells and is indispensable for bone-building.[7] Many physiological functions are also associated with Zn; it is essential to growth, immune function and tissue maintenance.[7] Recently, Huang *et al.*[8] have described the immunomodulatory osteoinductive effects of the Zn-loaded bioactive ceramics. They have shown that this biomaterial plays a dual role in endogenous bone regeneration and presented a novel concept of coupling spontaneous osteogenesis with favorable osteoimmunomodulation characteristics. Notably, Zn can relocate Ca by modifying the calcium-dependent processes. In general, the changes in the functions affected by the incorporation of metallic elements are dose-dependent and lead to upregulation or downregulation of biological processes.[7]

In our previous *in vivo* tests and proteomic studies, we have demonstrated that the sol–gel coatings formulated with tetraethyl orthosilicate (TEOS) and methyltrimethoxy orthosilicate (MTMOS) have excellent osteoinductive and biocompatibility properties.[5] To develop new coatings with OIM properties we used our previous experience to synthesize sol–gel coatings formulated with TEOS and MTMOS co-doped with two elements with a main role in bone homeostasis, Ca and Zn. A thorough characterization, *in vitro* testing and proteomic study of the pathways triggered by the Ca-doped materials with different concentrations of Zn were conducted to assess the OIM response.

2. Experimental

2.1. Sol–gel synthesis and sample preparation

The sol–gel hybrid coatings were synthesized using MTMOS and TEOS alkoxysilanes in a molar ratio of 7 : 3 in a 2-propanol (50% v/v) medium, following the method previously optimized by our team.[9] The various formulations contained different amounts of $CaCl_2$ and $ZnCl_2$ previously dissolved in an aqueous solution (Table 1). To examine the effect of the two cations, the content of $CaCl_2$ was fixed at 0.5 wt% (the proportion established stablished in our previous study[6]). $ZnCl_2$ was added to obtain three different coatings containing Zn at 0.5, 1 and 1.5 wt%. A basic formulation without salts (MT) and the coating doped with Ca only (MT-Ca) were used as controls. The sol–gel mixtures were kept under stirring for 1 h and 1 h at rest. Then, the different substrates were coated. First, sandblasted and acid-etched grade-4 Ti discs of 10 mm and 12 mm diameter (1 mm thick) were used.[5] The 10 mm discs were employed in *in vitro* assays and the 12 mm diameter discs in the proteomic

and physicochemical analyses. The synthesized sol–gel formulations were applied onto the discs using a dip-coater (KSV DC; KSV NIMA, Espoo, Finland). The immersion was performed at 60 cm min^{-1}, after 1 min, the samples were removed at a 100 cm min^{-1}. To evaluate the hydrolytic degradation of the materials and the cations kinetic release, the coatings were applied onto glass-slides. The glass surface was first conditioned in HNO_3 (25% v/v) in an ultrasonic bath (Sonoplus HD 3200; Bandelin Electronic, Berlin, Germany) for 20 min at 30 W. Afterwards, the slides were cleaned by sonication in distilled water and dried at 100 °C. At this point, the glass substrates were coated using a casting method. For the chemical characterization, free films of different sol–gel compositions were obtained by pouring 3 mL of each sol into non-stick Teflon molds.

Finally, all the samples were cured (2 h at 80 °C). All the reagents were purchased from Sigma-Aldrich (St. Louis, MO, USA).

2.2. Physicochemical characterization

A Fourier Transform Infrared Spectrometer (FTIR; Thermo Nicolet 6700, Thermo Fisher Scientific, NY, US) with an attenuated total reflection system (ATR) was used to study the sol–gel materials. The spectra were measured in the 4000–400 cm^{-1} range. A solid-state silicon nuclear magnetic resonance spectroscope (^{29}Si-NMR; Bruker 400 Avance III WB Plus spectrometer, Billerica, MA, US) with a cross polarization magic angle spinning (CP-MAS) probe for solid samples was used to study the crosslinking degree of the obtained sol–gel structures. The measurements were performed using the standard Bruker pulse sequence: 79.5 MHz frequency, 55 kHz spectral width, 2 ms contact time and 5 s delay time. The spinning frequency was 7.0 kHz. The coatings applied onto Ti discs were morphologically characterized employing a scanning electron microscope (SEM; Leica-Zeiss LEO, Leica, Wetzlar, Germany). The samples were sputtered with platinum before the evaluation to increase their conductivity. The surface roughness was measured with an optical profilometer PLm2300 (Sensofar, Barcelona, Spain). Three independent samples of each material were studied, and three measurements were performed for each sample. The results were expressed as the average value of Ra (arithmetic average roughness parameter). The sample wettability was evaluated using an automatic contact angle meter OCA 20 (Dataphysics Instruments, Filderstadt, Germany). Ultrapure water drops (about 10 μL) were deposited on the discs at 27.5 μL s^{-1}. The drop angles were analyzed using SCA 20 software (DataPhysics Instruments). Six samples were tested (two drops were deposited for each sample) for each condition. The hydrolytic degradation of the coatings was determined by measuring the mass loss during the incubation in 50 mL of distilled water at 37 °C. The results were expressed as the percentage (%) of the initial mass lost. The samples were evaluated after 7, 14, 28, 42 and 56 days of incubation. Three distinct samples were studied for each condition. The Zn^{2+} and Ca^{2+} release kinetics were obtained by using an inductively coupled plasma mass spectrometer (Agilent 7700 Series ICPMS, Agilent Technologies, Santa Clara, CA, US). The coatings were incubated in ddH$_2$O at 37 °C

Table 1 Nomenclature and composition of the formulated sol–gel materials. The mass percentages of $CaCl_2$ and $ZnCl_2$ were calculated with respect to the total amount of alkoxysilane

Nomenclature	$CaCl_2$ (wt%)	$ZnCl_2$ (wt%)
MT	0	0
MT-Ca	0.5	0
MT-Ca0.5Zn	0.5	0.5
MT-Ca1Zn	0.5	1
MT-Ca1.5Zn	0.5	1.5

for 28 days. After 2, 4, 6, 8, 24, 72, 168, 336, 504 and 672 h of incubation, liquid aliquots of 0.5 mL were analyzed. Three individual samples were evaluated for each condition.

2.3. Evaluation of *in vitro* cell responses

2.3.1. Cell culture. *In vitro* tests were carried out using mouse calvaria osteosarcoma (MC3T3-E1) cells and mouse murine macrophage (RAW 264.7). The cells were maintained at 37 °C in an incubator with 90% humidity and 5% CO_2. The MC3T3-E1 culture medium was composed of low-glucose DMEM (Gibco, Life Technologies, Thermo Fisher Scientific, NY, USA) supplemented with 1% penicillin/streptomycin (Gibco) and 10% FBS (Gibco). To stimulate osteogenic differentiation, the culture medium was replaced, after 24 h, with osteogenic medium (DMEM, 1% of penicillin/streptomycin, 10% FBS, ascorbic acid (50 μg mL^{-1}) and 100 mM β-glycerol phosphate). The medium was changed every two days. The RAW 264.7 cells medium was composed of high-glucose DMEM (Gibco) supplemented with 1% penicillin/streptomycin and 10% FBS.

2.3.2. Biomaterial cytotoxicity. Cytotoxicity was assessed following the ISO 10993-5:2009 (Annex C) standard and samples were prepared according to the ISO 10993-12:2012. MC3T3-E1 cells were seeded into 96-well NUNC plates (Thermo Fisher Scientific) at a density of 1×10^5 cells cm^{-2} and maintained in a humidified incubator. At the same time, the materials were incubated in the cell-culture medium for serum extraction. After 24 h, the cells were exposed to the material extract for another day. The CellTiter 96$^{\circledR}$ Proliferation Assay (MTS; Promega, Madison, WI) was used according to the manufacturer's guidelines. For controls, unexposed cells (negative control) and cells incubated with latex (positive control) were used. The material was considered cytotoxic when the cell viability fell below 70%.

2.3.3. Alkaline phosphatase activity in osteoblasts. The osteogenic properties of the synthesized materials were first evaluated by measuring the ALP activity, following the protocol described by Araújo-Gomes et al.[10] MC3T3-E1 cells were seeded onto the coated samples in 48-well NUNC plates (Thermo Fisher Scientific) at a density of 1.75×10^4 cells cm^{-2}. After 7 and 14 days of culture, the cells were immersed in lysis buffer (0.2% Triton X-100, 10 mM Tris–HCl, pH 7.2) for 10 min at 4 °C. Then, 100 μL of *p*-NPP (1 mg mL^{-1}) in the substrate buffer (50 mM glycine, 1 mM $MgCl_2$, pH 10.5) was added to 100 μL of the sample. After 2 h of incubation in the dark, the absorbance at 405 nm was measured using a microplate reader. Alkaline phosphatase activity was calculated using the standard curve (*p*-nitrophenol in 0.02 mM sodium hydroxide), and activity was normalized to protein content obtained using the Pierce BCA assay kit (Thermo Fisher Scientific).

2.3.4. Proteomic analysis of the adsorbed protein layer. The protocol described before[5] was followed for the proteomic analysis of the adsorbed protein layer. The materials were incubated for 3 h (37 °C, 5% CO_2) in 24-well NUNC plates (Thermo Fisher Scientific) with 1 mL of human serum from male AB plasma (Sigma-Aldrich). This incubation time was stablished based on previous studies.[11] Then, to eliminate the non-adsorbed proteins, the materials were washed five times with ddH$_2$O and

once with the wash buffer (100 mM NaCl, 50 mM Tris–HCl, pH 7.0). The adsorbed protein layer was extracted with the elution buffer (Thiourea 2 M, Urea 7 M, 4% Chaps, DTT 200 mM). Four independent replicates of each material were analyzed and each replicate was prepared by pulling the extracts of protein layers adsorbed onto four discs. The total protein concentration in the serum was obtained using the Pierce BCA Protein Assay Kit (Thermo Fisher).

The analysis of the proteins was performed employing the electrospray tandem mass spectrometry, using a nanoACQUITY UPLC (Waters, Milford, MA, USA) coupled to an Orbitrap XL (Thermo Electron, Bremen, Germany) as described previously.[5] Each sample was analyzed in a quadruplicate. Differential protein analysis was carried out using the PEAKS platform (Bioinformatics Solutions Inc., Waterloo, Canada). The protein classification by function was carried out using the DAVID Go annotation program (https://david.ncifcrf.gov/) and the UniProt classification system (https://www.uniprot.org/).

2.3.5. Statistical analysis. The physicochemical characterization results and *in vitro* assays data (considering normal distribution and equal variance) were analyzed using one-way variance analysis (ANOVA) with Tukey's *post hoc* test. To confirm the results, the Student's *t*-test was performed after the ANOVA analysis. The data were expressed as means ± standard error. Statistical analysis was performed using GraphPad Prism 5.04 software (GraphPad Software Inc., La Jolla, CA, USA) and considered significant at $p \leq 0.05$. The asterisk (*) indicates differences between the MT and the ion-doped coatings, and the rhombus (♦) indicates differences between the Ca-doped and the CaZn-doped materials.

For the proteomic analysis data, the Student's *t*-test was conducted to evaluate differences between the MT and MT-Ca and CaZn samples using the Progenesis data analysis software. Proteins were considered differentially expressed if their levels differed significantly ($p \leq 0.05$) and the ratio changed by at least 1.5 in either direction (increased or decreased).

3. Results

3.1. Physicochemical characterization

As described above, the materials (Table 1) were synthesized following the sol–gel method and their final chemical structure was analyzed by FTIR and ^{29}Si-NMR spectrometry (Fig. 1). Fig. 1a shows their FTIR spectra. There were no significant differences attributable to the addition of salts to the base material MT. The bands associated with the polysiloxane chain vibration (770, 1020 and 1125 cm^{-1}) indicate the formation of Si–O–Si bonds[6] during the condensation reaction. The band at 950 cm^{-1} is due to Si–OH bonds, characteristic of non-condensed groups.[6] The bands at 1265 and 2980 cm^{-1}, are associated with Si–C and C–H bonds, respectively; they reflect the methyl group integrity maintenance in the sol–gel structure after the synthesis. Similarly, the incorporation of salts in MT did not cause significant differences in the ^{29}Si-NMR spectra (Fig. 1b). The characteristic signals of the MTMOS trifunctional
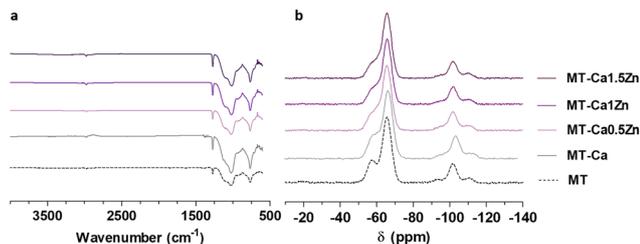
8196 | *J. Mater. Chem. B*, 2023, **11**, 8194–8205

This journal is © The Royal Society of Chemistry 2023

Fig. 1 (a) FT-IR spectra and (b) ^{29}Si-NMR of the various sol–gel materials.

Fig. 3 (a) Sol–gel coatings hydrolytic degradation kinetic; (b) Zn^{2+} and (c) Ca^{2+} ions release from the various doped coatings. Data are represented as mean $\pm$ SE.

precursor (called T units)[12] were detected at the -50 and -75 ppm range; while the signals of the TEOS tetrafunctional precursor (called Q units)[12] appeared between -97.5 and -120 ppm.[13] Peaks at -62 and -70 ppm are associated with the formation of T^2 and T^3 species in the network. The peaks at -99, -106 and -116 ppm are linked to Q^2, Q^3 and Q^4 crosslinked structures, respectively.[5] At the end of the reaction, T^3 was the highest chemical shift for MTMOS and Q^3 for TEOS.

As we can see in Fig. 2a–f, sol–gel coatings cover thoroughly the roughness of the sand blasted Ti discs. A slight porosity appeared in doped coatings increasing as the Zn content increased (Fig. 2c′–f′′). Nevertheless, profilometry measurements (Fig. 2g) did not show any statistically significant differences (although the co-doped samples showed the lowest values). Contact angle measurements were carried out to evaluate changes in surface wettability due to the addition of Ca^{2+} and Zn^{2+} (Fig. 2h). A statistically significant increase (of approximately 25°) in contact angle was observed after incorporating 0.5% of $CaCl_2$ into the sol–gel network. The materials containing both the Ca and Zn ions and Ca-only materials showed similar wettability values.

Fig. 3 shows the kinetics of coatings degradation and the release of each ion in a water medium. As shown in Fig. 3a, the undoped sample, MT, showed the slowest mass loss, increasing throughout the test to a value of 38% at 56 days. However, the salt-containing samples degraded faster during the first 10 days of the experiment and progressively reached a plateau at mass loss of 40–50%. Increased doping augmented the extent of degradation. Fig. 3b and c show the Zn and Ca-ion release,
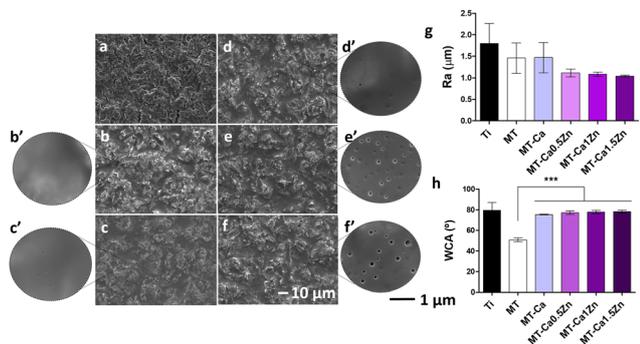
respectively. In all cases, we can observe a release burst after the 24 first hours; the steady-state was reached close to 0.1 ppm for the MT-Ca0.5Zn formulation, 0.3 ppm for the MT-Ca1Zn and 0.6 for the MT-Ca1.5Zn sample. The Ca release was similar for all the formulations, increasing slightly with an increase in the Zn content, reaching values between 0.3 ppm and 0.4 ppm.

3.2. *In vitro* tests results

3.2.1. Cytotoxicity and ALP activity. Cytotoxicity results are depicted in Fig. 4a. Cells cultured with any of the tested sol–gel biomaterials showed viability considerably higher than the 70%, *i.e.* none of the materials was cytotoxic. The effects of the materials on mineralization expressed as ALP activity are shown in Fig. 4b. After 7 days, a significant increase in ALP activity was observed for the MT-Ca and CaZn co-doped compositions compared to MT. In contrast, after 14 days, all these materials caused a significant decrease in ALP activity in comparison with MT and MT-Ca.

3.2.2. Relative gene expression. Two gene expression factors, ALP and TGF-β, were examined to evaluate the OIM capacities of the new sol–gel materials after 7 and 14 days of incubation. Fig. 5a demonstrates that only the cell exposed to Ca1.5Zn show a significantly higher expression of ALP than those grown with MT and MT-Ca; the expression increased dramatically after 14 days. Moreover, incorporating Ca into the MT network increased the expression of the TGF-β gene at 14 days (Fig. 5b). However, the addition of Zn ions caused a significant decrease in TGF-β expression in cultures with CaZn-doped coatings in comparison with MT-Ca or MT at 14 days.

The TNF-α gene expression, associated with inflammatory responses, was significantly enhanced in macrophages cultured with MT-Ca for 2 days (relative to MT). In contrast, reduced

Fig. 2 SEM images of uncoated Ti (a), MT (b), MT-Ca (c), MT-Ca0.5Zn (d), MT-Ca1Zn (e), MT-Ca1.5Zn. Scale bars: (a–f) 10 μm and (c′–f′) 1 μm. Profilometry measurements of the various sol–gel coatings and sandblasted Ti as a reference (g). Contact angle (WCA) results (h). The asterisk (*) indicates differences between MT and the ion doped-samples; (***) = $p \leq 0.001$.
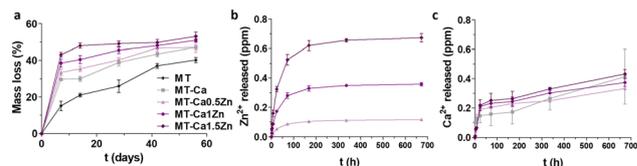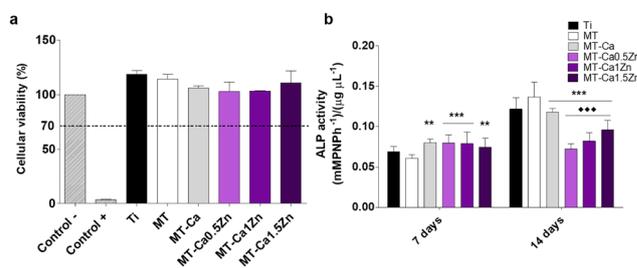

Fig. 4 (a) Cellular viability of MC3T3-E1 on the synthesized materials after 24 h and (b) ALP activity in MC3T3-E1 at 7 and 14 days. Results are shown as mean $\pm$ SE. Asterisks indicate differences between MT and the ion doped-coatings: (**) = $p \leq 0.01$; (***) = $p \leq 0.001$; and the rhombus indicates differences between the CaZn-doped coatings and MT-Ca ($\blacklozenge\blacklozenge\blacklozenge$) = $p \leq 0.001$.

This journal is © The Royal Society of Chemistry 2023

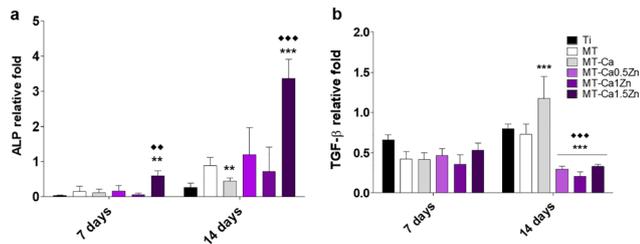*J. Mater. Chem. B*, 2023, **11**, 8194–8205 | **8197**

Fig. 5 Relative gene expression of (a) alkaline phosphatase (ALP) and (b) transforming growth factor (TGF)-β on MC3T3-E1 at 7 and 14 days. Data are normalized in relation to blank (wells without any material) with the $2^{-\Delta\Delta C_t}$ method. Results are shown as mean ± SE. The asterisk (*) indicates differences between MT and the ion doped-coatings: (**) = $p \leq 0.01$; (***) = $p \leq 0.001$; and the rhombus indicates differences between the MTCa and the CaZn-doped materials: (♦♦) = $p \leq 0.01$; (♦♦♦) = $p \leq 0.001$.

expression of this gene was observed during this period for MT-Ca0.5Zn and MT-Ca1Zn in comparison with Ca-only coating. After 4 days, the cells grown with MT Ca and all the co-doped materials showed increased TNF-α expression (relative to MT; Fig. 6a). After 2 days, the expression of the anti-inflammatory marker TGF-β (Fig. 6b) increased in cultures with MT-Ca and MT-Ca1.5Zn in comparison with MT. Co-doping with the Zn and Ca reduced the expression of this marker for MT-Ca0.5Zn and MT-Ca-1Zn in comparison with MT-Ca. However, a significantly increased expression was observed for MT-Ca1.5Zn. After 4 days, all the cultures with the co-doped materials showed significantly higher expression values than the cells grown with MT or MT-Ca.

3.3. Proteomic results

The nLC-MS/MS analysis of eluted proteins identified 183 different proteins adsorbed onto the distinct materials. Table 2 (ST2, ESI†) shows the proteins differentially adsorbed on the Ca and CaZn materials in comparison with the MT. A comparative analysis of proteins found on the CaZn and MT-Ca coatings was performed to examine the effect of Zn ions in the coating on protein adsorption (Table 3 – ST3, ESI†).

Moreover, Table 2 summarizes the results presented in ST2 and ST3 (ESI†). This table displays the differential adsorption of the key proteins for the regenerative process on grouped
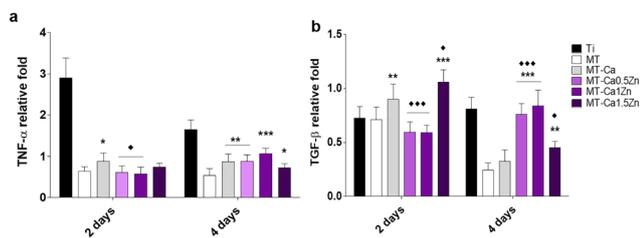

Fig. 6 Relative gene expression of (a) tumor necrosis factor (TNF)-α and (b) transforming growth factor (TGF)-β on RAW264.7 at 2 and 4 days. Data were normalized in relation to blank (wells without any material) with the $2^{-\Delta\Delta C_t}$ method. Results are shown as mean ± SE. The asterisk (*) indicates differences between MT and the ion doped-coatings: (*) = $p \leq 0.05$; (**) = $p \leq 0.01$; (***) = $p \leq 0.001$; and the rhombus indicates differences between the MT-Ca-doped and the CaZn-doped materials: (♦) = $p \leq 0.05$; (♦♦♦) = $p \leq 0.001$.

formulations, to highlight how their adsorption patterns are influenced by both the ions addition to MT and the Zn content in the mixture CaZn.

The ST2 (ESI†) shows that the ratio of adsorbed proteins rises with the increase in the Zn content. Moreover, the higher the Zn ion content, the fewer proteins with reduced affinity are adsorbed. The data in the ST3 (ESI†) (comparison with MT-Ca) show that the effect of increasing the amount of Zn is similar, but the only differentially adsorbed proteins are those with increased adsorption. The number of such proteins is much higher if the MT is used as the reference rather than the MT-Ca material (i.e., 79 in ST2 and 20 in ST3, ESI†).

As expected, almost all the proteins showing differential adsorption relative to MT-Ca material (ST3, ESI†) appear on the list of differentially adsorbed proteins obtained in the comparison with MT (ST2, ESI†). Looking at the common proteins appearing on both lists, we observed that two proteins, histidine-rich glycoprotein (HRG) and plasminogen (PLMN) had the highest ratio values among the Zn-containing samples. The HRG adsorption ratio grows from 2.76 for MT-Ca0.5Zn to 6.85 for MT-Ca1.5Zn (ST3, ESI†). However, in incubations with MT Ca material, the adsorption of this protein is not changed. The HRG is associated (UniProt database) with the regulation of many processes such as immune complex and pathogen clearance, cell chemotaxis, cell adhesion, angiogenesis, coagulation and fibrinolysis. Therefore, it could be linked to several biological functions, mainly blood coagulation and cell adhesion. The other protein with the highest ratio, PLMN, is also related to blood coagulation and, hence, to tissue regeneration. The ratio for this protein rises with increasing Zn content, reaching the value of 5.25 for the MT-Ca1.5Zn formulation. However, its adsorption appears reduced on the material without Zn. The FA5 protein, showing reduced affinity to MT-Ca and increased adsorption to MT-Ca0.5Zn and MT-Ca1.5Zn samples, is another protein related to blood coagulation that appears in the two lists. This function of this protein depends on Ca-binding and are linked to hemostasis.

Some of the differentially adsorbed proteins common to the two lists (ST2 and ST3, ESI†) are related to immune response. These are SAA1, APOL1, IGHM and CLUS, involved in the innate immune system, and two apolipoproteins, APOC4 and APOE,[14,15] associated with the adaptative immune response (APOE is linked to osteogenic effects). The SAA1 and APOL1 have the highest ratios: the SAA1 level is reduced on MT-Ca (the ratio of 0.17) but it has the ratios around 3 for MT-Ca1Zn and MT-Ca1.5Zn (ST2, ESI†). The APOL1 shows the highest ratio, 2.07, for MT-Ca1.5Zn compared to MT-Ca cultures (ST3, ESI†). IGHM is differentially adsorbed onto the material with 1.5% Zn (ratio of 2.02, compared to MT-Ca); its adsorption to all the Zn-containing surfaces is higher than to the MT material. CLUS has increased affinity to all the new formulations and is differentially adsorbed to the Ca-material (with the highest ratio of 3.28). In comparisons with MT-Ca (ST3, ESI†), this protein is preferentially adsorbed to only two Zn-containing materials, MT-Ca1Zn (ratio of 1.52) and MT-Ca1.5Zn (ratio 1.91). The adsorption of the two apolipoproteins associated with the adaptative immune response is strongly affected by adding Zn. APOC4 occupies one of the highest

8198 | J. Mater. Chem. B, 2023, 11, 8194–8205

This journal is © The Royal Society of Chemistry 2023

Table 2 Summary of dysregulated protein patterns adsorbed onto the sol–gel coatings. Comparison are made gathering doped materials with increasing amounts of Zn with respect to MT and MTCa. Relevant biological processes (blood coagulation, immune response and tissue regeneration) are represented

Dysregulated adsorbed proteins	Formulation	Biological function		
		Blood coagulation	Immune response	Tissue regeneration
DOWN adsorbed proteins comparing to MT	MT-Ca	FA5, PLMN[a]	CO8G, **APOC4**[b], **KV320**[b], SAA1	PKP1
	MT-Ca, MT-Ca0.5Zn, MT-Ca1Zn, MT-Ca1.5Zn	THRB, ANT3, FA10, FA12[a], FA9, CBPB2, PROC		PCOC1, **VTNC**[c], IBP4, **PRG4**[c]
	MT-Ca0.5Zn, MT-Ca1Zn, MT-Ca1.5Zn	—	—	—
	MT-Ca1Zn, MT-Ca1.5Zn		FCN2	
	MT-Ca1.5Zn	IPSP	IGLL5	TGM1
UP adsorbed proteins comparing to MT	MT-Ca		CLUS, CO7	**TSK**[b], APOF, HRG[a], APOA4, APOA1
	MT-Ca, MT-Ca0.5Zn, MT-Ca1Zn, MT-Ca1.5Zn	HRG[a]		LG3BP, GELS, APOM
	MT-Ca0.5Zn, MT-Ca1Zn, MT-Ca1.5Zn	APOH	APOL1, CO5, IGHM, CFAH CO6, CO9, KNG1[a], HPTR[a]	
	MT-Ca1Zn, MT-Ca1.5Zn	KNG1[a], HPTR[a]	**LV147**[b], CO4A, IGHD, C4BPA, IGHG4	HABP2, HBD, GPX3, PLMN[a]
	MT-Ca1.5Zn	PLMN[a]		PLMN[a]
UP adsorbed proteins comparing to MT-Ca	MT-Ca0.5Zn, MT-Ca1Zn, MT-Ca1.5Zn	HRG[a], PLMN[a]	**KVD33**[b], CLUS, SAA1	PLMN[a]
	MT-Ca1Zn, MT-Ca1.5Zn		APOE[a], CD14	HRG[a], APOA4
	MT-Ca1.5Zn			**APOE**[ac], GPX3

[a] Proteins with two main functions. [b] Bold: adaptive immune response function. [c] Bold: bone regeneration function.

positions in ST3 (ESI†), showing significant changes in adsorption, with ratio values of 2.36 and 3.01 for MT-Ca0.5Zn and MT-Ca1.5Zn formulations, respectively. The affinity of APOE to MT-Ca coating is reduced (ratio 0.43) in comparison with MT; it shows an increase in adsorption only for the formulation with the highest Zn content (ratio 1.69) compared to MT-Ca.

Some other proteins involved in regeneration processes appear on both comparison lists. Among these, 3 antioxidant proteins, GPX3, HBD and APOA4, are differentially adsorbed onto the material with the highest Zn concentration. The GPX3 protein shows a ratio of 3.53 for MT-Ca1.5Zn. HBD, whose activity is metal-ion dependent, has a ratio of 2.78 for MT-Ca1.5Zn. APOA4 shows higher adsorption levels on MT-Ca1Zn and MT-Ca1.5Zn than on MT-Ca and is found in larger quantities on all the doped materials than on MT.

VTNC and other 2 proteins, FETUA and PRG4, are directly involved in bone regeneration. VTNC plays an important role in cell–cell adhesion, extracellular matrix (ECM) organization, and other cellular processes. This protein shows a significantly increased adsorption on all the surfaces compared to MT. However, in comparison with MT-Ca, its adsorption is only higher on the MT-Ca0.5Zn formulation (ratio of 1.77). PRG4 shows an increased deposition only for the MT-Ca1Zn material with a ratio of 2.19, relative to MT-Ca and reduced adsorption on all the surfaces in comparison with MT. FETUA, a protein related to biological function of mineral balance, has increased affinity to MT-Ca1Zn.

There are many more proteins differentially adsorbed onto the new sol–gel ion-doped materials in comparison with the bare MT. Adding metallic ions to the sol–gel material reduces the adsorption of a considerable number of blood coagulation-related proteins. Specifically, ion-doping affects the adsorption of proteins THRB, ANT3, FA9, FA10, FA12, CBPB2 and PROC on all the formulations and the deposition of IPSP protein on MT-Ca1.5Zn. Among these, the THRB, FA9, FA10 and PROC are Ca proteins involved in proteolytic processes. In contrast, FA12 and CBPB2 are Zn-binding proteins associated with the same processes of blood coagulation and fibrinolysis. ANT3 and IPSP are involved in heparin-binding and IPSP inactivates serine proteases and has a hemostatic role in the blood plasma. The number of coagulation related proteins showing augmented adsorption grows with rising Zn content. Thus, apart from already mentioned HRG and PLMN, increased amounts of APOH, KNG1 and HPTR proteins are deposited on Zn-containing materials. APOH participates in blood coagulation processes through plasminogen activation and KNG1 is a Zn-binding protein. The HPTR, a heparin-binding protein, is also involved in the acute inflammatory response. An inhibitor of serine proteases, A1AT, blocks trypsin, chymotrypsin and plasminogen activator and is one of the seven differentially adsorbed to MT-Ca1Zn coating.

Many other proteins triggering immune response were differentially adsorbed onto the coatings. Most of these proteins are related to inflammatory, innate or adaptive immune responses; their numbers increase with increasing Zn content in the films. Some of the proteins with reduced adsorption

This journal is © The Royal Society of Chemistry 2023

J. Mater. Chem. B, 2023, **11**, 8194–8205 | **8199**

Table 3 Summary of enriched functions associated to blood coagulation, immune response and tissue regeneration detected by DAVID analysis

	Formulation	Dysregulation	Annotation clusters number	Proteins count	DAVID enriched functions		
					Blood coagulation	Immune response	Tissue regeneration
Differentially adsorbed proteins compared with MT	MT-Ca	DOWN	6	21	– Heparin binding – Fibrinolysis – Serine protease – Blood coagulation – GLA domain	– Amyloidosis	– ECM – EGF-like domain – Lipid transport
		UP	3	6	—	—	– Lipid transport – Glycoprotein
	MT-Ca0.5Zn	DOWN	4	19	– Heparin binding – Fibrinolysis – Serine protease – Blood coagulation	– Immunoglobulin domain	– EGF-like domain – Disulphide bond – Glycoprotein
		UP	6	16	– Blood coagulation	– Complement activation – Innate immune response	– Disulphide bond – Glycosylation – Lipid metabolism
	MT-Ca1Zn	DOWN	2	13	– Serine protease – Blood coagulation – GLA domain		– Disulphide bond – Glycoprotein – EGF-like domain
		UP	9	29	– Blood coagulation – Haemostasis	– Regulation of complement activation – Complement activation – Innate immune response – Membrane attack complex	– EGF-like domain – Disulphide bond – Lipid transport
	MT-Ca1.5Zn	DOWN	4	15	– Heparin binding – Haemostasis – Serine protease – Blood coagulation – GLA domain		– EGF-like domain – Disulphide bond – Glycoprotein
		UP	12	28	– Heamostasis – Blood coagulation	– Regulation of complement act – Complement activation – Innate immune response – Membrane attack complex – B cell receptor signaling pathway – Immunoglobulin receptor bind. – Inflammatory response	– EGF-like domain – Disulphide bond – Lipid transport
Differentially adsorbed proteins compared with MT-Ca	MT-Ca0.5Zn	UP	2	8	– Haemostasis – Blood coagulation	– Immunoglobulin domain	– Disulphide bond – Glycoprotein
	MT-Ca1Zn		3	8	—	– Immunoglobulin domain – Adaptative immune response	– Disulphide bond – Glycoprotein
	MT-Ca1.5Zn		4	14	—	– Immunoglobulin domain	– Lipid transport – Cell membrane

(compared to MT) are CO8G, FCN2, the acute phase protein SAA2, and the immunoglobulins KV320, IGLL5, KV127, KV106, KVD40, IGHG1 and IGHG3. Among the proteins that set off the complement activation system, CO8G participates in the classical and alternative pathways, and FCN2, a Ca-binding protein, participates in the lectin pathway. Moreover, a cluster of proteins related to immunity (with increased adsorption in doped coatings in comparison with MT) was also found. The cluster contains the immunoglobulins IGJ, LV147, IGHG4 and IGHD and the complement activation system proteins CFAB, CO5, CO4A, CO6, CO7, CO9. The proteins C4BPA, IC1, CFAI and CFAH with an essential role in maintaining a well-balanced immune response by modulating complement activation, also belong to this group. Other cluster members are A1AG1 and A1AG2 glycoproteins (modulating the activity of the immune system) and the apolipoproteins APOM and APOA1, with anti-oxidant and inflammation regulation functions.

Additionally, some proteins deposited onto metal-doped materials intervene in tissue regeneration functions; most are differentially adsorbed onto all these materials (relative to MT). Among the proteins with reduced adsorption, the PKP1 promotes the cell–cell adhesion. PCOC1 enhances procollagen C-proteinase activity. TGM1 is a Ca-binding protein involved in the cell cycle regulation, and IBP4 has a role in cell growth. In the group with increased adsorption, we found the TSK protein, important for the bone growth, and the APOF, related to cell adhesion. Apart from HRG, these two proteins are among the most abundant, and their absorption increases with Zn concentration. The antioxidant proteins APOA4 and APOA1, related to cholesterol homeostasis, are also found on all the materials. Two Ca-dependent proteins, GELS and HABP2, and the LG3BP protein are associated with cell adhesion. The APOM protein participates in tissue regeneration *via* cholesterol homeostasis,[15] and PEDF, contributes to the maintenance of bone homeostasis and inhibits angiogenesis.

Some proteins were only differentially adsorbed onto the CaZn sol–gel coatings in comparison with Ca-MT. Among these, the CD14 protein and immunoglobulins KVD33 and KV117 (involved in the immune response) augmented their adsorption levels. Similarly, the DSC1 protein, associated with cell–cell adhesion, showed increased adsorption on the Ca–Zn coatings.

The DAVID Go annotation analysis was also used to examine the dose-dependent effect of Ca- and Zn-doping on protein adsorption to the tested coating materials (Table 3). The program gathers all the proteins involved in the same biological process and provides information on significantly enriched functions, according to the categorical Gene Ontology data, protein domain and biochemical pathway membership.[16] Table 3 lists all GO (UP_KEYWORDS) functions identified as enriched and related to bone tissue regeneration. The total number of identified annotation clusters of functions and the protein count (down and upregulated) are also shown. The comparison between Ca-doped and co-doped (Ca and Zn) materials shows an increase in the number of annotation clusters (from 9 to 16) and proteins (from 27 to 43) as we increase Zn concentration. Thus, calcium addition reduces mostly the adsorption of proteins associated with blood coagulation mechanisms and tissue regeneration. The addition of Zn to the Ca-material affects mainly the immune response proteins in a dose-dependent manner. The membrane attack complex function appears for materials with 1% and 1.5% of Zn. An inflammatory response cluster is observed for the material with the highest concentration of Zn. Thus, some functions associated with enhancing the immune/inflammatory response are seen after increasing the Zn content in the coatings. However, the complement system activation function is also found for MT-Ca1Zn, and some immune functions are linked to proteins with reduced adsorption. Functions associated with serine protease appear for all the formulations.

The analysis using a different database, *i.e.* the GOTERM_BP_DIRECT, shed new light on the type of processes associated with various important biological functions such as the serine protease regulation. Thus, the proteins associated with serine-type endo-peptidase activity and proteolysis appear upregulated after adding Ca to MT material. The same processes appear differentially downregulated for MT-Ca, MT-Ca0.5Zn and MT-Ca1.5Zn. At the same time other processes linked to protease activity, such as inhibition of endopeptidase activity, appear upregulated for MT-Ca1Zn and MT-Ca1.5Zn.

4. Discussion

Many scientific studies have demonstrated that incorporating a combination of metal ions into bone-implant biomaterials affects the immune response. This suggests that it should be possible to design an advanced bone material with an optimal combination of elements.[3] Si, Ca and Zn have some immunor-egulatory properties, affecting the inflammation processes in a dose-dependent manner. The release of Si complexes to the ECM and their presence on the material surface may also have dose-dependent stimulatory effects on the bone cells and cartilage tissue systems.[17] Similarly, the Zn and Ca trace elements are key both in bone formation and repair[18] and in hemostasis.[7]

These are some of the reasons that encourage us to design new hybrid silicon-based sol–gel materials incorporating the Ca and Zn ions. Our previous studies have demonstrated that Ca participates in the coagulation process but is also involved in the inflammatory response.[6] Moreover, Zn has a strong dose-dependent effect on immunological, coagulative, and regenera-tive functions.[19] Thus, to exploit these diverse properties, we decided to use a low concentration of Ca (0.5%) in all the formulations and add various proportions of Zn. In this way, new treatments based on the Ca + Zn were developed with the aim of evaluating the biological effect of the mixture. We used the FTIR and ^{29}Si-NMR to prove that all the sol–gel formula-tions condensed to form a crosslinked hybrid material. The weight loss studies demonstrated that these sol–gel coatings were degradable in contact with water and released the Ca and Zn ions. The application of the coatings on the Ti surface implies a decrease in its roughness, since the sol–gel network was deposited on the Ti irregularities, attenuating its topogra-phy. The Ra changed from 1.8 µm for Ti to 1.5 µm for MT.

This journal is © The Royal Society of Chemistry 2023

J. Mater. Chem. B, 2023, 11, 8194–8205 | 8201

On the other hand, the addition of ions did not show statistical differences between the different Ra values of the doped coatings with respect to MT. In parallel, the Ti modification with MT supposed an increased hydrophilicity. However, the doping of the coatings with ions led to higher contact angle values, without reaching the level obtained for Ti. Rough Ti surfaces were reported to generate an osteogenic micro-environment able to promote osteoblast differentiation and inhibit osteoclast activation.[20] Regarding the surface hydrophilicity, increased wettability has been shown to enhance interaction between an implant surface and its biologic environment, promoting bone cell maturation and differentiation.[21] In this sense, it is difficult to establish the effect of these two parameters on the biological results obtained, since the variation of both variables, together with the chemical modification due to the incorporation of bioactive ions, were carried out simultaneously.

As Mestres et al.[4] have reported in their review of the evaluation of the OIM properties of biomaterials, the most common and accepted in vitro testing methods include the exposure of different key cell types to regulatory factors in the conditioned medium. The MT-Ca1.5Zn composition provoked a higher ALP gene expression in osteoblasts cultured with this material compared to those cultured with the Ti, MT and MT-Ca controls. In fact, MT-Ca showed a reduced ALP expression with respect to MT at 14 days. In parallel, both the MT-Ca and the MT-CaZn samples gave rise to a higher ALP activity compared to the treatment without ions (MT) at 7 days. In addition, a decrease in this marker was detected at 14 days in the coatings doped with Ca and CaZn with respect to MT, finding statistical differences also between the results for MT-Ca and the MT-CaZn compositions. This behavior could be associated with an acceleration of the mineralization process with a maximum shift in ALP activity to shorter times because of the cations added to the sol–gel network. In a previous work,[19] we reported the ability of Zn^{2+} to promote ALP gene expression and the osteoblast mineralization; so the Ca and Zn ion mixture maintained this effect, despite the result found for MT-Ca. Here, the expression of the TGF-β gene was dramatically decreased on the Ca-Zn co-doped sol–gels after 14 days. However, Ca-MT showed an increased expression of this gene, and Zn-containing materials were also able to promote the TGF-β expression.[19] As this molecule participates in the osteoblast recruitment, proliferation and differentiation, this reduction in its expression could result in an inhibitory effect on the bone formation when the two ions are released simultaneously.

The expression of pro-inflammatory TNF-α and anti-inflammatory TGF-β genes in macrophages were affected Ca–Zn. The TNF-α expression showed a small but significant increase after 4 days of incubation. The expression of the anti-inflammatory marker TFG-β increased markedly during the same period in comparison with the bare coating and Ca-only formulation (the lowest increase was seen for the MT-Ca1.5Zn coating). The results are quite consistent with the biological response of macrophages exposed to materials doped with only Ca or Zn. Exposure to sol–gel coatings enriched with Ca increases TNF-α expression and the secretion of this cytokine in a Ca dose-dependent manner.[6] The addition of Zn causes a clear anti-inflammatory effect, reducing the expression and secretion of TNF-α and increasing the expression of TFG-β.[19] Chen et al.[22] have studied nutrient element-based bioceramic coatings on titanium. They have concluded that a high concentration of Zn in the conditioned medium may be a key reason for the inhibition of macrophage growth and dampening of the inflammatory response. These authors have also reported that decreasing the concentration of Ca results in anti-inflammatory effects. Huang et al.[8] have incorporated Zn^{2+} into β-tricalcium phosphate/poly(L-lactic acid) scaffold and described that scaffolds loaded with 10% Zn has the best capacity to spontaneously promote osteogenic differentiation of periosteum-derived progenitor cells. The scaffolds loaded with 5% of Zn had the strongest ability to modulate the M2 polarization of macrophages. Many other studies, inspired by the similarity of the bioceramics to the natural bone tissue, have examined the effect of partial substitution of Ca by other cations and reported the osteogenic effects of Zn.[23,24] However, they all used highly Ca-rich materials, such as bioceramics or calcium phosphate or bioglasses. Therefore, it seems reasonable to assume that the Ca-based biomaterials are very different from the Si-based sol–gel materials that have similar concentrations of charged ions.

The presence of two different ions in the formulation might produce unexpected in vitro responses due to their potential antagonist effects. We must consider that, although the two cations have the same charge and thus could be involved in similar reactions or polar interactions, their atomic masses (Ca: 40.078 and Zn: 65.38) and, hence, their atomic volumes are very different. This could affect the proteins folding and associations[25] and, as a result, the cell behavior. Joh et al.,[26] who have designed a minimalist model for Zn^{2+}/H^+ co-transport membrane protein, have observed that their model was capable of moving first-row transition metal ions, Zn^{2+} and Co^{2+}, across the phospholipid bilayer, but not the hard divalent metal cation, Ca^{2+}. This adds weight to the importance of using proteomics to improve our knowledge of metallic ion-doped biomaterials interactions.

PEAKS comparative analysis identified different serum proteins adsorbed on the tested materials, showing specific patterns depending on the presence and amount of Zn^{2+}. Some of these proteins attracted our attention because they were also encountered on the Zn-only materials examined in our previous work.[19] For example, HRG adsorbed onto the Zn-doped coatings, and its amounts increased on the materials with higher Zn content. The HRG protein binds heparin and heparin/glycosaminoglycans in a zinc dependent manner and is involved in platelet activation, aiding both the coagulation and regeneration processes.[27] Two apolipoproteins, APOC4 and APOL1, associated with the adaptative and innate immune systems, respectively, were also common to the coatings prepared with Zn salts in the study cited above. The APOC4 adsorption is reduced on Ca-containing materials, and both these proteins appear in increased amounts on the coatings containing Zn, except for MT-Ca1Zn. This could indicate an improved immune response to this last material. Likewise, CLUS can increase its affinity to the materials doped with only Ca or Zn.[6,19] Here, we found that its adsorption was augmented on all the Ca–Zn formulations. In this case, the CLUS protein, a complement cascade

8202 | J. Mater. Chem. B, 2023, 11, 8194–8205

This journal is © The Royal Society of Chemistry 2023

inhibitor, could act as an anti-inflammatory factor; it might modulate the immune/inflammatory response to achieve the correct tissue regeneration.[3] Moreover, other 7 proteins adsorbed to the materials tested here showed a clear Zn dependency: PLMN, APOH, CO5, IGHM, CFAH, LG3BP, GELS and APOM. These proteins participate either in blood coagulation, immune response, or regeneration processes.

PLMN, which appears in protein clusters on all the materials, showed reduced adsorption to Ca materials but increased affinity to Zn-containing formulations. This protein is essential to many regeneration processes and is particularly known for its role in fibrinolysis (UniProt). The immunoglobulins IGKC and HRG, which appear on the three Zn-containing materials, are involved both in the immune response and regeneration. The four proteins (SAA1, APOA4, CLUS and KVD33) found in the protein clusters on the two materials with the highest Zn-content are important players in the OIM processes too. The bioactivity of SAA1 protein is under study, however, Zhou et al.[28] have observed that small changes in its structure diminish its pro-inflammatory activity. These changes also convey anti-inflammatory properties and strongly suppress inflammatory markers, such as TNF-α, in the macrophages. Such potential structural changes could be one of the reasons for apparent inconsistencies in the in vitro tests results. Experiments using fetal membranes have indicated a possible role for SAA1 in the ECM remodeling via the NF-κB and MAPK pathways.[29] CLUS can also trigger many biological processes linked to the positive regulation of NF-kB transcription factor activity and cell morphogenesis. Remarkably, other authors have affirmed that Zn can both stimulate bone formation and repress bone resorption, this could be achieved by inhibiting the activation of NF-kB signal transduction induced by TNF-α and RANKL.[30] As this signaling pathway is necessary for osteoclastogenesis but suppresses osteoblastogenesis, we find some discrepancies between our results and the data found in the literature. Nevertheless, our previous study[19] did not find any difference in the RANKL expression with the addition of Zn, similarly to other authors.[31] The conclusion was that the effect of Zn-enriched materials on osteoclastogenesis could depend on added Zn. Moreover, we should remember the potential effect of Ca in our coatings on many of these biological processes. The ECM holds a set of molecules that can directly activate the MAPK or are needed for MAPK function (key in bone development and homeostasis). Calcium, one of the main constituents of bone ECM, increases the MC3T3 proliferation by activating two MAPKs, ERK and p38; its chemical blockage inhibits the proliferative effect.[32] The proteins associated with regeneration and coagulation functions were found in increased amounts on the materials containing the mixture of ions (compared to the MT-Ca surfaces). Clear adsorption patterns depending on the Zn content were identified for APOE, HRG and PLMN and two proteins with antioxidant functions APOA4 and GPX3.

Various proteins involved in bone formation were also preferentially adsorbed onto specific Ca–Zn enriched coatings without showing a clear ion dose-dependency. Among these, the FETUA and PON1 proteins appear in associations with biological processes for the materials with the highest Zn concentrations. The FETUA protein regulates endochondral ossification by inhibiting mineralization and lipid binding.[33] PON1 is a Ca-dependent glycoprotein with a proposed role in bone metabolism. It preserves high-density lipoproteins functions and metabolizes biologically active phospholipids in oxidized low-density lipoproteins.[34] The DSC1 protein, linked to the Ca-ion storage activity and associated with bone regeneration via cell–cell adhesion appears in MT-Ca0.5Zn, the formulation with the lowest Zn content. In contrast, the other two proteins related to regeneration, APOA1 and TSK, adsorb to the MT-Ca coating. It is worth mentioning that PRG4 and VTNC, associated with osteogenic functions (UniProt), adsorbed in larger amounts to materials containing Zn than to MT-Ca; we can conclude that Zn increases their affinity to these surfaces.

It seems difficult to match these data with the results of the in vitro tests. However, the DAVID Go analysis clarified the effects of Ca and Zn on the biological processes they trigger, indicating the important role of these ions in the healing process. Thus, we observed that small amounts of one ion, i.e., 0.5% of Ca^{2+}, stimulated a cascade of biological responses, upregulated or downregulated. Adding 0.5% of Zn^{2+} affected only a few more responses; however, the number and type of upregulated protein packets increased as more Zn^{2+} was added. This highlights the ease of tuning biomaterials using metal ions essential for bone regeneration. Consequently, we need to study the diffusion of these ions in the surrounding tissues to understand their effects (desirable or detrimental) on the cellular responses.[18] It is worth mentioning that the serine protease-related functions (found for MT-Ca and Zn-containing formulations) appear augmented for the negative regulation of endopeptidase activity and its inhibition, for the materials with the highest concentration of Zn. This function is associated with collagen protection and mineralization and it is frequently attributed to the presence of Zn.[35] Likewise, the membrane attack functions are related to the antibacterial properties of Zn.[36] Thus, adding a small amount of Zn to the Ca-containing formulation mainly strengthens the association with the blood coagulation pathways triggered by calcium. Increased Zn content changes the immune response, and the highest Zn concentration enhances almost all the biological processes observed at low Zn levels. We can see that 1.5% of Zn is needed to augment the association with the processes linked to lipid metabolism. This is important since this metabolism is controlled during the adaptive and innate immune responses.[14] Similarly, we observed a major role for protein glycosylation. This is a highly complex post-translational modification affecting various biological processes, such as protein folding, signaling, trafficking, cell–cell interactions and immune response.[37] Here, the polymorphism could be attributed to slight protein modifications during the test development or alternative splicing (a molecular mechanism modifying pre-mRNA constructs prior to translation) provoked by Zn addition.[38]

5. Conclusion

The study shows that adding metal ions to biomaterials may affect many biological processes triggered by implantation. Our

This journal is © The Royal Society of Chemistry 2023

J. Mater. Chem. B, 2023, **11**, 8194–8205 | 8203

results demonstrate the highly tunable nature of sol–gel materials and their usefulness as a basic material for experimental studies. This flexibility resulted very useful for examining the interplay between the immune and bone-forming processes due to mixtures of Ca and Zn bioactive ions. These cations were able to promote ALP gene expression and osteoblast mineralization when are combined in a sol–gel network. Notably, proteomics allowed to observe that Ca–Zn doping increased the adsorption of immune system proteins onto the coating surfaces. In addition, Zn^{2+} was capable of controlling the pro-inflammatory responses associated with Ca ions, as well as promoting the adsorption of proteins able of regulating the immune response such as CLUS and APOE; showing these elements an osteoimmunomodulatory role. In this sense, the study clearly demonstrates the importance of introducing proteomics as an essential tool in the development of functional biomaterials; such materials should be capable of inducing the appropriate material–host interactions. Proteomics is also very useful for examining the processes affecting bone generation, such as coagulation, angiogenesis or ECM formation.

Author contributions

IGA: data curation, investigation FRG: writing – review & editing, data curation, investigation AC: data curation, investigation MA: data curation, investigation FE: resources, investigation JS: formal analysis, funding acquisition, project administration IG: formal analysis, funding acquisition, project administration MG: writing – original Draft, formal analysis, funding acquisition, project administration.

Conflicts of interest

There are no conflicts to declare.

Acknowledgements

Notes and references

1 A. M. Negrescu and A. Cimpean, *Materials*, 2021, **14**, 1357.
2 J. R. Arron and Y. Choi, *Nature*, 2000, **408**, 535–536.
3 Z. Chen, T. Klein, R. Z. Murray, R. Crawford, J. Chang, C. Wu and Y. Xiao, *Mater. Today*, 2016, **19**, 304–321.
4 G. Mestres, S. S. D. Carter, N. P. Hailer and A. Diez-Escudero, *Acta Biomater.*, 2021, **130**, 115–137.
5 F. Romero-Gavilan, N. Araújo-Gomes, A. M. Sánchez-Pérez, I. García-Arnáez, F. Elortza, M. Azkargorta, J. J. M. de Llano, C. Carda, M. Gurruchaga, J. Suay and I. Goñi, *Colloids Surf., B*, 2018, **162**, 316–325.
6 F. Romero-Gavilán, N. Araújo-Gomes, A. Cerqueira, I. García-Arnáez, C. Martínez-Ramos, M. Azkargorta, I. Iloro, F. Elortza, M. Gurruchaga, J. Suay and I. Goñi, *J. Biol. Inorg. Chem.*, 2019, **24**, 563–574.
7 B. Dalisson and J. Barralet, *Adv. Healthcare Mater.*, 2019, **1900764**, 1–22.
8 X. Huang, D. Huang, T. Zhu, X. Yu, K. Xu, H. Li, H. Qu, Z. Zhou, K. Cheng, W. Wen and Z. Ye, *J. Nanobiotechnol.*, 2021, **19**, 1–20.
9 M. Martinez-Ibañez, I. Aldalur, F. J. Romero-Gavilán, J. Suay, I. Goñi and M. Gurruchaga, *J. Non. Cryst. Solids*, 2018, **481**, 368–374.
10 N. Araújo-Gomes, F. Romero-Gavilán, I. García-Arnáez, C. Martínez-Ramos, A. M. Sánchez-Pérez, M. Azkargorta, F. Elortza, J. J. M. de Llano, M. Gurruchaga, I. Goñi and J. Suay, *J. Biol. Inorg. Chem.*, 2018, **23**, 459–470.
11 F. Romero-Gavilán, A. M. Sanchez-Pérez, N. Araújo-Gomes, M. Azkargorta, I. Iloro, F. Elortza, M. Gurruchaga, I. Goñi and J. Suay, *Biofouling*, 2017, **33**, 676–689.
12 A. R. G. E. Lippmaa, M. Maegi, A. Samoson and G. Engelhardt, *J. Am. Chem. Soc.*, 1980, **102**, 4889–4893.
13 F. Romero-Gavilán, J. Carlos-Almeida, A. Cerqueira, M. Gurruchaga, I. Goñi, I. M. Miranda-Salvado, M. H. Vaz Fernandes and J. Suay, *Prog. Org. Coatings*, 2020, **147**, 105770.
14 A. Reboldi and E. Dang, *F1000Research*, 2018, **7**, 1647.
15 B. Wang and P. Tontonoz, *Nat. Rev. Endocrinol.*, 2018, **14**, 452–463.
16 G. Dennis, B. T. Sherman, D. A. Hosack, J. Yang, W. Gao, H. C. Lane and R. A. Lempicki, *Genome Biol.*, 2003, **4**, R60.
17 A. M. Pietak, J. W. Reid, M. J. Stott and M. Sayer, *Biomaterials*, 2007, **28**, 4023–4032.
18 E. O'Neill, G. Awale, L. Daneshmandi, O. Umerah and K. W. H. Lo, *Drug Discovery Today*, 2018, **23**, 879–890.
19 A. Cerqueira, F. Romero-Gavilán, I. García-Arnáez, C. Martinez-Ramos, S. Ozturan, I. Iloro, M. Azkargorta, F. Elortza, R. Izquierdo, M. Gurruchaga, I. Goñi and J. Suay, *Mater. Sci. Eng., C*, 2021, **121**, 1–10.
20 B. D. Boyan, S. Lossdörfer, L. Wang, G. Zhao, C. H. Lohmann, D. L. Cochran and Z. Schwartz, *Eur. Cells Mater.*, 2003, **6**, 22–27.
21 G. Zhao, A. L. Raines, M. Wieland, Z. Schwartz and B. D. Boyan, *Biomaterials*, 2007, **28**, 2821–2829.
22 Z. Chen, J. Yuen, R. Crawford, J. Chang, C. Wu and Y. Xiao, *Biomaterials*, 2015, **61**, 126–138.
23 X. Luo, D. Barbieri, N. Davison, Y. Yan, J. D. De Bruijn and H. Yuan, *Acta Biomater.*, 2014, **10**, 477–485.
24 X. Li, Y. Sogo, A. Ito, H. Mutsuzaki, N. Ochiai, T. Kobayashi, S. Nakamura, K. Yamashita and R. Z. LeGeros, *Mater. Sci. Eng., C*, 2009, **29**, 969–975.
25 Y. Von Hansen, I. Kalcher and J. Dzubiella, *J. Phys. Chem. B*, 2010, **114**, 13815–13822.
26 N. H. Joh, G. Grigoryan, Y. Wu and W. F. DeGrado, *Philos. Trans. R. Soc. B Biol. Sci.*, 2017, **372**, 20160214.

8204 | *J. Mater. Chem. B*, 2023, **11**, 8194–8205

This journal is © The Royal Society of Chemistry 2023

27 Y. Wang, Z. Li, F. Mo, Z. Gu and Q. Hu, *Nano Today*, 2021, **40**, 101281.

28 H. Zhou, M. Chen, G. Zhang and R. D. Ye, *J. Immunol.*, 2017, **199**, 1105–1112.

29 Y. W. Wang, W. S. Wang, L. Y. Wang, Y. R. Bao, J. W. Lu, Y. Lu, C. Y. Zhang, W. J. Li, K. Sun and H. Ying, *Am. J. Reprod. Immunol.*, 2019, **81**, 1–9.

30 M. Yamaguchi and M. N. Weitzmann, *Mol. Cell. Biochem.*, 2011, **355**, 179–186.

31 K. Yusa, O. Yamamoto, M. Iino, H. Takano, M. Fukuda, Z. Qiao and T. Sugiyama, *Arch. Oral Biol.*, 2016, **71**, 162–169.

32 E. Rodríguez-Carballo, B. Gámez and F. Ventura, *Front. Cell Dev. Biol.*, 2016, **4**, 1–20.

33 L. Brylka and W. Jahnen-Dechent, *Calcif. Tissue Int.*, 2013, **93**, 355–364.

34 B. J. Kim, S. Y. Kim, Y. S. Cho, B. J. Kim, B. G. Han, E. K. Park, S. H. Lee, H. Y. Kim, G. S. Kim, J. Y. Lee and J. M. Koh, *Exp. Mol. Med.*, 2011, **43**, 71–81.

35 M. Toledano, R. Osorio, M. Vallecillo-Rivas, E. Osorio, C. D. Lynch, F. S. Aguilera, R. Toledano and S. Sauro, *J. Mech. Behav. Biomed. Mater.*, 2021, **114**, 104232.

36 H. Yang, X. Qu, W. Lin, D. Chen, D. Zhu, K. Dai and Y. Zheng, *ACS Biomater. Sci. Eng.*, 2019, **5**, 453–467.

37 T. Pitti, C. T. Chen, H. N. Lin, W. K. Choong, W. L. Hsu and T. Y. Sung, *Sci. Rep.*, 2019, **9**, 1–11.

38 T. V. Ramanouskaya and V. V. Grinev, *Mol. Genet. Genomics*, 2017, **292**, 1175–1195.

This journal is © The Royal Society of Chemistry 2023

J. Mater. Chem. B, 2023, **11**, 8194–8205 | **8205**